ISSN 1062-8738, Bulletin of the Russian Academy of Sciences: Physics, 2010, Vol. 74, No. 6, pp. 870–874. © Allerton Press, Inc., 2010.
Original Russian Text © A.S. Nikitin, A.A. Khamzin, A.A. Lukmanov, A.S. Sitdikov, 2010, published in Izvestiya Rossiiskoi Akademii Nauk. Seriya Fizicheskaya, 2010, Vol. 74, No. 6, pp. 910–914.

Kinematic Moments of Inertia of $A = 74$ nuclei at Presence of Neutron-Proton Interactions

A. S. Nikitin, A. A. Khamzin, A. A. Lukmanov, and A. S. Sitdikov

Kazan State Power Engineering University, Kazan, 420066 Russia
e-mail: airat_vm@rambler.ru

Abstract—Quasiparticle and collective characteristics of the isotopic triplet of ^{74}Rb, ^{74}Kr and ^{74}Se were studied in the Hartree–Fock–Bogolyubov approximation, in combination with a forced-rotation model depending on the rotation frequency at moderate spins. It was shown that for ^{74}Rb, the first intersection in yrast occurs due to an aligning of the spins of the n–p pair, which leads to backbending in the behavior of the moment of inertia at $\hbar\Omega \simeq 0.25$ MeV. In the last two even–even nuclei, the smooth behavior of the moment of inertia is explained by an enhancement of the competition between the $T = 1$ and $T = 0$ modes at $\hbar\Omega > 0.5$ MeV.

DOI: 10.3103/S1062873810060298

INTRODUCTION

It is known that the specificity of the features of the ground and excited states of atomic nuclei is first of all conditioned by their proton–neutron composition and the complex nature of the interaction between particles. Nucleon–nucleon pair correlations are among the most interesting of these despite their apparent triviality. Although we may at present consider the proton–proton and neutron–neutron pairing to be well-studied, the question of isoscalar pairing/correlations remains open [1, 2]. Nuclei with $N \approx Z$ (and, of course, with $N = Z$), in which the identical orbitals with $T = 0$ are filled by protons and neutrons [3], are the most interesting objects of study from both the experimental and theoretical points of view. Such filling occurs in lighter nuclei (with $A < 40$) [4], the ground (gr) states of which are formed in the isoscalar mode.

However, an increase in atomic mass leads to an enhancement of the role of the Coulomb and spin–orbit interactions, leading in turn to the violation of isotopic symmetry. As a result, the isovector $T = 1$ component, which competes with the isoscalar $T = 0$ mode, starts to dominate inside the nuclei [3]. Such competition occurs mainly in transition nuclei with $A \approx 70 - 80$, the main feature of which is the coexistence of forms with oblate and prolate deformations at low spins.

At present, the amount of spectroscopic information [5–8] on the low- and high-spin states of such nuclei is quite large. This opens the possibility of studying them as they rotate, and the aim of this work is therefore to study the quasiparticle spectrum and kinematic moments of inertia of the gr states of an isobaric triplet (an odd–odd ^{74}Rb nucleus and even–even ^{74}Kr, and ^{74}Se nuclei) at moderate spins in the cranking model, in combination with the Hartree–Fock–Bogolyubov (HFB) method.

FRM + HFB FORMALISM

We start from the FRM Hamiltonian [9, 10], determined in the rotating coordinate system as follows:

$$\hat{H}' = \hat{H} - \sum_{\tau} \lambda_\tau \hat{N}_\tau - \Omega \hat{J}_x, \quad (1)$$

where $\hat{H}$ is the full many-particle Hamiltonian in the laboratory system, $\hat{N}_\tau$ is the operator of the number of particles (protons, $\tau = Z$ and neutrons, $\tau = N$), λ_τ is the chemical potential, Ω is the angular rotation frequency, and $\hat{J}_x$ is the projection of the total angular moment of nucleus on the *ox* axis.

The residual interactions in the deformed mean field are taken as monopole pairing and np interactions. The full Hamiltonian $\hat{H}$ can then be written as

$$\hat{H} = \sum_k \varepsilon_k (\hat{a}_k^+ \hat{a}_k + \hat{a}_{\bar{k}}^+ \hat{a}_{\bar{k}}) - \frac{1}{4}\sum_\tau G_\tau \hat{P}_\tau^+ \hat{P}_\tau - \frac{1}{2}\sum_{\beta\gamma\xi\rho} \langle \beta\gamma | V_{\rm np} | \xi\rho \rangle \hat{a}_\beta^+ \hat{a}_\gamma^+ \hat{a}_\xi \hat{a}_\rho, \quad (2)$$

where ε_k is the single-particle energies in the distorted mean field; $\hat{a}_k^+$, $\hat{a}_k$ ($a_{\bar{k}}^+$, $\hat{a}_{\bar{k}}$) are the operators of the creation and annihilation of particles, respectively, in the $k(\bar{k})$ state; G_τ is the constant of pairing($\tau \in$ n,p);

$\hat{P}_\tau^+ = \sum_{k\in\tau} \hat{a}_k^+ \hat{a}_{\bar{k}}^+$ is the operator of pairing, and the $\hat{a}_k^+$ and $\hat{a}_{\bar{k}}^+$ operators are coupled by a time reversal by the $\hat{K}$ relation

$$\hat{a}_{\bar{k}}^+ = \hat{K}\hat{a}_k^+\hat{K}^{-1}.$$

Here, $\sum_{\beta\gamma\xi\rho} \langle\beta\gamma|V_{\rm np}|\xi\rho\rangle$ are non-antisymmetrized two-particle matrix elements of np interaction, and Greek indices run over all of the ensemble of single-particle states. We write the potential of np interactions as the sum

$$V_{\rm np} = V_W + V_\sigma, \quad (3)$$

consisting of the Wigner

$$V_W = -4\pi(1-\alpha)V_\Gamma e^{-\frac{|r_{\rm n}-r_{\rm p}|^2}{r_g^2}}, \quad (4)$$

and spin–spin

$$V_\sigma = -4\pi\alpha V_\Gamma e^{-\frac{|r_{\rm n}-r_{\rm p}|^2}{r_g^2}}\sigma_{\rm n}\sigma_{\rm p}, \quad (5)$$

parts, where $r_g = 1.4$ fm, and α and V_Γ (the depth of the potential well) are constants [11].

The invariance of the Hamiltonian $\hat{H}'$ with respect to the $\hat{R}_x(\pi)$ symmetry ($\hat{R}_x(\pi) = \exp(i\pi\hat{J}_x)$ is the operator of the rotation around the x-axis at angle π) allows us to select the basis of the single-particle states from the condition that these states be eigenvectors of the $\hat{R}_x(\pi)$ operator:

$$e^{i\pi\hat{J}_x}\begin{pmatrix}\hat{c}_k^+\\ \hat{c}_{\bar{k}}^+\end{pmatrix}e^{-i\pi\hat{J}_x} = \mp\begin{pmatrix}\hat{c}_k^+\\ \hat{c}_{\bar{k}}^+\end{pmatrix}. \quad (6)$$

This basis with respect to the $\hat{R}_x(\pi)$ symmetry satisfies the relations

$$\hat{R}_x(\pi)|k\rangle_G = -i|k\rangle_G, \quad \hat{R}_x(\pi)|\bar{k}\rangle_G = i|\bar{k}\rangle_G. \quad (7)$$

Such a $|\ \rangle_G$ basis such was first introduced by Goodman in [12], and is therefore called the Goodman basis. By assuming the invariance of np interaction with respect to rotations and time reversal and using relations (6) and (7), we can show that the two-particle potential $V_{\rm np}$ in the Goodman basis can be written as

$$V_{\rm np} = \frac{1}{2}\sum_{klpn}\Big[\langle kl|V_{\rm np}|pn\rangle_G\left(\hat{c}_k^+\hat{c}_l^+\hat{c}_n\hat{c}_p + \hat{c}_{\bar{k}}^+\hat{c}_{\bar{l}}^+\hat{c}_{\bar{n}}\hat{c}_{\bar{p}}\right) + \langle kl|V_{\rm np}|\overline{pn}\rangle_G\left(\hat{c}_k^+\hat{c}_{\bar{l}}^+\hat{c}_n\hat{c}_p + \hat{c}_k^+\hat{c}_l^+\hat{c}_{\bar{n}}\hat{c}_{\bar{p}}\right)$$
$$+\left(\langle k\bar{l}|V_{\rm np}|p\bar{n}\rangle_G - \langle k\bar{l}|V_{\rm np}|\bar{n}p\rangle_G\right)\left(\hat{c}_k^+\hat{c}_{\bar{l}}^+\hat{c}_{\bar{n}}\hat{c}_p + \hat{c}_{\bar{k}}^+\hat{c}_l^+\hat{c}_n\hat{c}_{\bar{p}}\right)\Big],$$

where, according to (3),

$$\langle kl|V_{\rm np}|pn\rangle_G = \langle kl|V_{({\rm np})W}|pn\rangle_G + \langle kl|V_{({\rm np})\sigma}|pn\rangle_G.$$

Expressions for the two-particle matrix elements are given in [11].

Below, using the Bogolyubov transformation, we move from single-particle $\hat{c}_k^+, \hat{c}_k$ operators to quasiparticle $\hat{\alpha}_k^+, \hat{\alpha}_k$ operators:

$$\hat{c}_k = \sum_i\left(A_k^i\hat{\alpha}_i + B_k^{\bar{i}}\hat{\alpha}_{\bar{i}}^+\right); \quad \hat{c}_k^+ = \sum_i\left(A_k^i\hat{\alpha}_i^+ + B_k^{\bar{i}}\hat{\alpha}_{\bar{i}}\right); \quad (8)$$

$$\hat{c}_{\bar{k}} = \sum_i\left(A_{\bar{k}}^{\bar{i}}\hat{\alpha}_i + B_{\bar{k}}^i\hat{\alpha}_i^+\right); \quad \hat{c}_{\bar{k}}^+ = \sum_i\left(A_{\bar{k}}^{\bar{i}}\hat{\alpha}_i^+ + B_{\bar{k}}^i\hat{\alpha}_i\right). \quad (9)$$

Having rewritten the Hamiltonian by using quasiparticle operators and transformations (8) and (9), we employ the variation principle to arrive at self-consistent equations for determining the A_k^i, $A_{\bar{k}}^{\bar{i}}$, $B_{\bar{k}}^i$ and $B_k^{\bar{i}}$ coefficients:

$$\begin{pmatrix}\aleph^{(1)}\Delta^{(1)}\\ \Delta^{(2)}\aleph^{(2)}\end{pmatrix}\begin{pmatrix}A_l^i\\ B_{\bar{l}}^i\end{pmatrix} = E_i\begin{pmatrix}A_l^i\\ B_{\bar{l}}^i\end{pmatrix} \quad (10)$$

and

$$\begin{pmatrix}\aleph^{(1)}\Delta^{(1)}\\ \Delta^{(2)}\aleph^{(2)}\end{pmatrix}\begin{pmatrix}B_l^{\bar{i}}\\ A_{\bar{l}}^{\bar{i}}\end{pmatrix} = E^{\bar{i}}\begin{pmatrix}B_l^{\bar{i}}\\ A_{\bar{l}}^{\bar{i}}\end{pmatrix}. \quad (11)$$

Expressions for the elements of matrices entering Eqs. (10) and (11) are given in [11].

DISCUSSION OF CALCULATION RESULTS

Within the above model, we solved self-consistent Eqs. (10) and (11) with the step $\Delta\hbar\Omega = 0.02$ MeV while limiting the basis by the states of shells with $N = 3,4$, which are completely sufficient for the considered ^{74}Rb, ^{74}Kr and ^{74}Se nuclei. We have enough spectroscopic information for these nuclei with regard to the energies of states with even and odd spins of positive and negative parity [5–8]. For the ^{74}Rb nucleus, e.g., the energies of the yrast states have been identified up to $I^\pi = 22^+$ for ^{74}Kr, to $I^\pi = 32^+$, and to $I^\pi = 22^+$, for ^{74}Se.

Figures 1–3 show the low-lying quasiparticle levels for the above nuclei in dependence on the $\hbar\Omega$. value. We can see in Fig. 1 for ^{74}Rb that a proton with the $\left[44\frac{9}{2}\frac{1}{2}\right]$ configuration is aligned at a rotation frequency of $\hbar\Omega \simeq 0.38$ MeV; a neutron with the same configuration, at a rotation frequency of $\hbar\Omega \simeq 0.45$MeV with the formation of an isoscalar $T = 0$ pair. The calculations were performed for the parameter of static deformation $\beta_{20} = 0.3$ [6], which in the calculations was

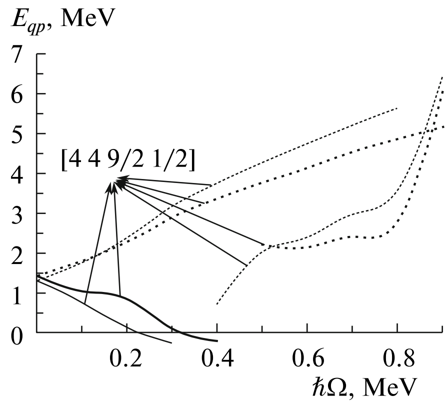

Fig. 1. Dependence of the energy of the calculated quasineutron (thick solid curves) and quasiproton (thin solid curves) E_{qp} levels on the rotation frequency $\hbar\Omega$ for the ^{74}Rb nucleus. The corresponding dashed lines denote states with the opposite signature.

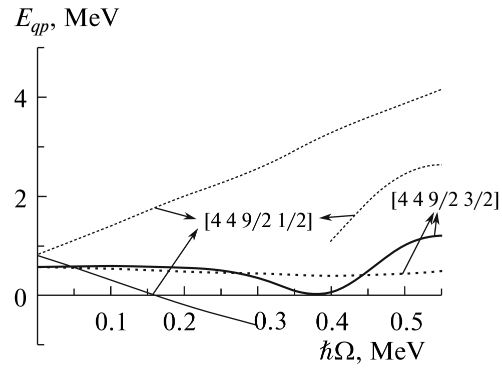

Fig. 2. The same as in Fig. 1, but for the ^{74}Kr nucleus.

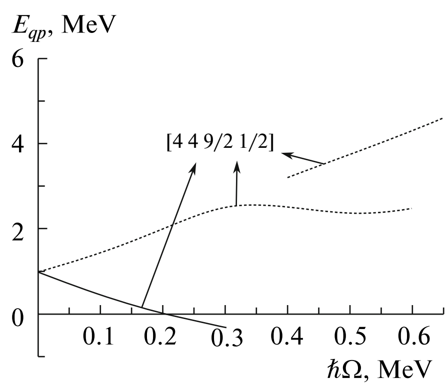

Fig. 3. The same as in Fig. 1, but for the ^{74}Se nucleus (the quasineutron level is not shown).

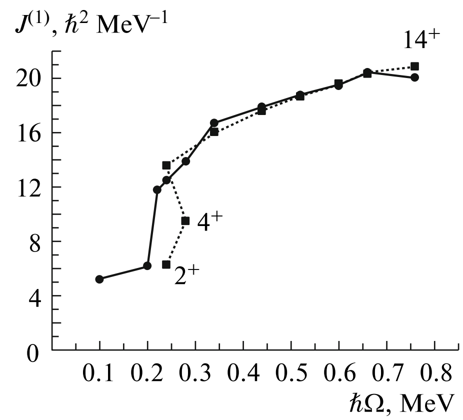

Fig. 4. Kinematic moment of inertia $J^{(1)}$ for yrast bands, in dependence on the angular frequency $\hbar\Omega$ for the ^{74}Rb nucleus. Squares—the experiment [6].

varied to 0.4. This allowed us to interpret the *gr* band consisting of the E_{2^+} and E_{4^+} levels as the $T = 1$ band crossing the aligned *s* band, starting E_{6^+} and having a $T = 0$ isospin (the neutron and proton, which reside initially in time-conjugated orbitals, occupy identical orbitals after alignment). However, our results differ somewhat from those in [6], where it was predicted on the basis of the quadrupolar core + valence nucleons model that this intersection occurs at a frequency of 0.2–0.3 MeV.

Figure 4 for this nucleus shows the values of the kinematic moment of inertia for the yrast band as compared to the experimental values: backbending occurs at a rotation frequency of $\hbar\Omega > 0.2$ MeV; in the experiment, it was observed at $\hbar\Omega_{cr} \simeq 0.28$ MeV. It should be noted that backbending at the moment of inertia occurs somewhat earlier than the alignment in the *s* band. A good test, sensitive to changes in the details of the nuclear spectrum, is the aligned angular moment $i(\Omega) = I(\Omega) - I_{ref}(\Omega)$ considered in [13]. The lower part of the *gr* band with the Harris inertial parameter $J_0 \simeq 8.5$ MeV^{-1} was selected as a reference (an unaligned inert band). It was shown that at $\hbar\Omega_{cr} \simeq 0.28$ MeV, the neutron–proton quasiparticle configuration $\nu(g_{9/2}) \otimes \pi(g_{9/2})$ aligns with $I_{max} = 2g_{9/2} \approx j_x = i(\Omega \geq \Omega_{cr})$.

Figure 2 shows the quasiparticle levels of the ^{74}Kr nucleus as calculated using the deformation parameter $\beta_{20} = 0.342$, which we estimated on the basis of the lifetime of the $E_{2^+}^{yrast}$ state. In our calculations, the β_{20} parameter was varied over a range of 0.342–0.360. According to our model, the alignment of the qua-

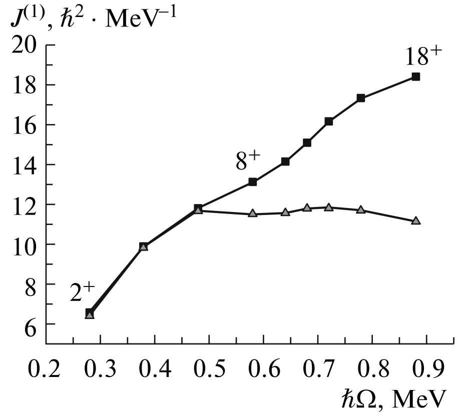

Fig. 5. The same as in Fig. 4, but for the ^{74}Kr nucleus.

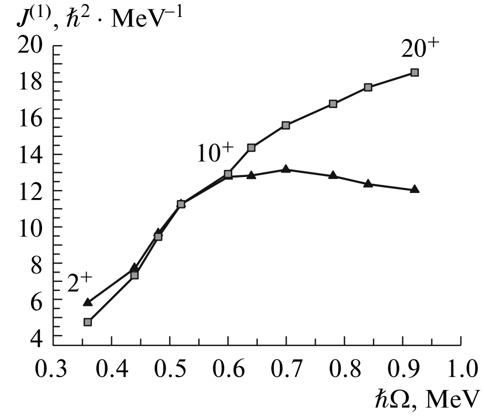

Fig. 6. The same as in Fig. 4, but for the ^{74}Se nucleus.

siproton $\left[44\frac{9}{2}\frac{1}{2}\right]$ configuration occurs in this nucleus at $\hbar\Omega \simeq 0.4$ MeV. As a result, the kinematic moment of inertia of the *gr* band starting at $\hbar\Omega \simeq 0.48$ MeV acquires the properties of a rigid rotor (Fig. 5). In this case, the alignment is smooth with no backbending. Within the above model, this can be explained as follows: At low rotation frequencies, the neutron and proton pairs are in isovector states with $T = 1$ and $T_z = \pm 1$ $\left[44\frac{9}{2}\frac{3}{2}\right]$ and $\left[44\frac{9}{2}\frac{1}{2}\right]$, respectively). At $\hbar\Omega \simeq 0.4$ MeV, the Coriolis forces align the angular moment of the proton, which transitions to the neutron level $\left[44\frac{9}{2}\frac{3}{2}\right]$ with the formation of an isoscalar n–p pair. Such an isoscalar pair is stable with respect to rotation, and the moment of inertia consequently changes little with the frequency. The theoretical behavior of the moment of inertia does not, however, correspond to the experimental values at $\hbar\Omega > 0.5$ MeV: according to the experiment, the moment of inertia increases. It should be noted that studying the nuclei of the given region becomes complicated due to the coexistence of two forms of deformation, which leads to the strong dependence of the calculation results on our model. As was shown in [7, 14], a mixing of states with different deformations (quadrupole, octupole, and hexadecapole) is possible at higher spins.

Similar behavior of the moment of inertia is characteristic for the ^{74}Se nucleus (Fig. 6). In the low-lying quasiproton state $\left[44\frac{9}{2}\frac{1}{2}\right]$, alignment occurs that leads to a smooth increase in the moment of inertia. Just as in the case of ^{74}Kr, however, no alignment is observed in the lowest quasineutron state (the quasineutron curve is not given in the figure). This is apparently a consequence of the proton's transition to the neutron level upon alignment and thus of the formation of the isoscalar n–p pair. The deformation parameter $\beta_{20} = 0.3$ was calculated on the basis of the lifetime values of the $E_{2^+}^{yrast}$ level and was varied between 0.3–0.4 in the calculations.

CONCLUSIONS

1. In an odd–odd ^{74}Rb nucleus, the initial alignment of the yrast band occurs due to the alignment of the angular moments of the odd neutron and odd proton, which occupy time-reversed orbitals (with $T = 1$, $T_z = 0$). This leads to the intersection of the *gr* band with $T = 1$ and the aligned *s* band with $T = 0$, such an intersection is thus diabatic.

2. In accordance with our model, a smooth alignment of the proton quasiparticle pair that has the smallest projection $\left(\left[44\frac{9}{2}\frac{1}{2}\right]\right)$ of the moment is observed in even–even ^{74}Kr, and ^{74}Se nuclei. This could indicate that when there is negligible competition between the $T = 1$ and $T = 0$ modes in the ground state, the isoscalar $T = 0$ mode starts to dominate as a result of the above alignment, and this leads to a weakening of the correlations in the neutron's Cooper pair. The further monotonous increase observed in the experiment in the moments of inertia of the last two nuclei (at $\hbar\Omega > 0.5$ MeV for ^{74}Kr and at $\hbar\Omega > 0.6$ MeV for ^{74}Se) can be explained by the alignment of the neutron's single-particle angular moment. In this work, however, we did not consider such single-particle alignment.

REFERENCES

1. Satula, W. and Wyss, R., *Acta Phys. Polonica B*, 2001, vol. 32, p. 2441.
2. Frauendorf, S., *Rev. Mod. Phys.*, 2001, vol. 73, p. 463.
3. Goodman, A.L., *Adv. Nucl. Phys.*, 1979, vol. 11, p. 263.
4. Goodman, A.L., *Phys. Rev. C*, 1999, vol. 60, p. 014311.
5. http://www.nndc.bnl.gov/nudat2/

6. Rudolph, D., Gross, C.J., Sheikh, J.A., et al., *Phys. Rev. Lett.*, 1996, vol. 76, p. 376.
7. Bender, M., Bonche, P., and Heenon, P.H., *Phys. Rev. C*, 2006, vol. 74, p. 024312.
8. Rudolf, D., Baktash, C., Gross, C.J., et al., *Phys. Rev. C*, 1997, vol. 56, p. 98.
9. Inglis, D.R., *Phys. Rev.*, 1955, vol. 97, p. 701.
10. Ring, P. and Chuck, P., *The Nuclear Many–Body Problem*, New York: Springer, 1980.
11. Sitdikov, A.S., Nikitin, A.S., and Khamzin, A.A., *Yad. Fiz.*, 2008, vol. 71, p. 262 [*Phys. At. Nucl.* (Engl. Transl.), 2008, vol. 71, p. 244].
12. Goodman, A.L., *Nucl. Phys. A*, 1974, vol. 230, p. 466.
13. Sitdikov, A.S., Nikitin, A.S., Khamzin, A.A., and Lukmanov, A.A., *Proc. 2nd Int. Conf. Current Problems in Nuclear Physics and Atomic Energy*, June 9–15 2008, part 1, p. 425.
14. Hinohara, N., Nakatsukasa, T., Matsuo, M., and Matsuyanagi, K., *Phys. Rev. C,* 2009, vol. 80, p. 014305.